Electronic Supplementary Information

Ultrafine Bimetallic Pt-Ni Nanoparticles Immobilized on 3-dimensional N-doped Graphene Networks: Highly Efficient Catalyst toward Dehydrogenation of Hydrous Hydrazine

Amit Kumar,[a] Xinchun Yang,[a] and Qiang Xu*[,a,b]

[a]Research Institute of Electrochemical Energy, National Institute of Advanced Industrial Science and Technology (AIST), 1-8-31 Midorigaoka, Ikeda, Osaka 563-8577, Japan

[b]AIST-Kyoto University Chemical Energy Materials Open Innovation Laboratory (ChEM-OIL), Yoshida, Sakyo-Ku, Kyoto 606-8501, Japan

1. Chemical and Materials

All the chemicals were obtained from the commercial sources and used without further purifications. Natural graphite (Alfa Aesar, >99.8%), sodium nitrate ($NaNO_3$, Wako Pure Chemical Industries Ltd., >98%), sulfuric acid (H_2SO_4, Wako Pure Chemical Industries Ltd., 98%), potassium permanganate ($KMnO_4$, Kishida Chem. Co., 99.3%), hydrogen peroxide (H_2O_2, Kishida Chem. Co., 30%), hydrochloric acid (HCl, Wako Pure Chemical Industries Ltd., >98%), melamine ($C_3H_6N_6$, Tokyo Chemical Industry Co. Ltd., 98%), formaldehyde (HCHO, Kishida Chem. Co., >99.5%), potassium tetrachloroplatinate(II) (K_2PtCl_4, Sigma Aldrich, >98%), nickel chloride hexahydrate ($NiCl_2 \cdot 6H_2O$, Tokyo Chemical Industry Co. Ltd., 99%), sodium hydroxide (NaOH, Wako Pure Chemical Industries Ltd., >98%), sodium borohyride ($NaBH_4$, Tokyo Chemical Industry Co. Ltd., 99%), and hydrazine monohydrate ($H_2NNH_2 \cdot H_2O$, Sigma Aldrich, 98%), were used as received. De-ionized (DI) water with a specific resistance of >18.0 MΩ·cm was used in all experiments.

2. Synthesis

2.1. Synthesis of graphene oxide (GO). Graphene oxide was synthesized using modified Hummers' method.[S1] In a typical reaction, natural graphite (1.0 g), sodium nitrate (1.0 g) and concentrated sulfuric acid (46.0 mL) were mixed and stirred at ice bath for 4 h, followed by gradual addition of $KMnO_4$ (6.0 g). After mixing, the ice bath was removed and the mixture was allowed to stir at room temperature for 2 h. Subsequently, 92 mL of pure water was added drop-wise and the suspension was heated at 98 °C for 15 min, followed by sequential addition of 200 mL of hot water and 20 mL of 33% H_2O_2. GO was obtained by centrifugation, washed with HCl and water several times and dried at 60 °C for 24 h.

2.2. Synthesis of 3-diemensional N-doped graphene networks (NGNs-850). Graphene oxide (0.60 g) was dispersed in 60 mL of DI water by ultrasonication and mixed with formaldehyde (4.0 mL, 37% wt) and melamine (1.40 g) under stirring at room temperature. The mixture was transferred to a 100 mL Teflon-lined autoclave and hydrothermally treated at 180 °C for 12 h. After cooling at room temperature, reduced graphene oxide/melamine formaldehyde resin (rGO/MFR) composite was obtained by centrifugation, washed with water and dried at 70 °C for 24 h under vacuum. Resulting rGO/MFR composite was subsequently calcined at 850 °C for 5 h under Ar atmosphere with a heating rate of 3 °C/min leading to the formation of NGNs-850. Similarly, NGNs-750, NGNs-800 and NGNs-900 have been obtained by calcination of rGO/MFR composite at 750, 800 and 900 °C, respectively, under analogous conditions.

2.3. Synthesis of 3-dimensional graphene networks (GNs). Graphene oxide (0.20 g), dispersed in 20 mL of DI water was transferred into a Teflon-lined autoclave and hydrothermally treated at 180 °C for 12 h. To maintain the 3-D architecture the resulting hydrogel was freeze-dried and subsequently calcined at 850 °C for 5 h under analogous conditions.

2.4. Syntheses of Pt_xNi_{1-x}/NGNs-850. The $Pt_{0.5}Ni_{0.5}$ nanoparticles supported on NGNs-850 was synthesized by a facile wet chemical impregnation reduction method. Typically, 10 mg of as-prepared NGNs-850 was ultrasonically dispersed in 5.0 mL of water and then mixed with an aqueous solution of K_2PtCl_4 (0.05 mmol) and $NiCl_2 \cdot 6H_2O$ (0.05 mmol). Subsequently, 25 mg of $NaBH_4$ dissolved in 1.0 mL of 2.0 M aqueous NaOH solution was added dropwise in the above suspension and vigorously stirred for 2.0 h leading to the deposition of $Pt_{0.5}Ni_{0.5}$ NPs on NGNs-850. The $Pt_{0.5}Ni_{0.5}$/NGNs-850 catalyst was obtained by centrifugation, washed with water and

used for catalytic reactions. The catalysts with different molar ratios of Pt and Ni were also prepared by a similar method using K_2PtCl_4 and $NiCl_2{\cdot}6H_2O$ in different amounts as follows: 0.1 mmol K_2PtCl_4 for $Pt_{1.0}Ni_{0.0}$/NGNs-850; 0.07 mmol K_2PtCl_4 and 0.03 mmol $NiCl_2{\cdot}6H_2O$ for $Pt_{0.7}Ni_{0.3}$/NGNs-850; 0.06 mmol K_2PtCl_4 and 0.04 mmol $NiCl_2{\cdot}6H_2O$ for $Pt_{0.6}Ni_{0.4}$/NGNs-850; 0.04 mmol K_2PtCl_4 and 0.06 mmol $NiCl_2{\cdot}6H_2O$ for $Pt_{0.4}Ni_{0.6}$/NGNs-850; 0.03 mmol K_2PtCl_4 and 0.07 mmol $NiCl_2{\cdot}6H_2O$ for $Pt_{0.3}Ni_{0.7}$/NGNs-850; and 0.1 mmol $NiCl_2{\cdot}6H_2O$ for $Pt_{0.0}Ni_{1.0}$/NGNs-850.

Additionally, $Pt_{0.5}Ni_{0.5}$/NGNs-750, $Pt_{0.5}Ni_{0.5}$/NGNs-800, $Pt_{0.5}Ni_{0.5}$/NGNs-900, $Pt_{0.5}Ni_{0.5}$/GNs and $Pt_{0.5}Ni_{0.5}$/graphene were also prepared by a similar procedure using supports NGNs-750, NGNs-800, NGNs-900, GNs and GO, respectively. For all the catalysts the total concentration of K_2PtCl_4 + $NiCl_2{\cdot}6H_2O$ was kept constant as 0.1 mmol. For characterization the prepared catalysts were dried under vacuum at 70 °C for 24 h.

3. Characterization

The Powder X-ray diffraction (P-XRD) patterns for as-synthesized samples were collected on Rigaku Ultima IV X-ray diffractometer with Cu-Kα radiation (λ = 0.15406 nm). The patterns were recorded between 5-90 ° with a step size of 0.02 ° and a scan speed of 10 ° min^{-1} at 40 kV and 40 mA. Fourier transform infrared spectroscopy (FTIR) analyses were carried out on Shimadzu IRTracer-100 spectrometer using ATR mode. The X-ray photoelectron spectroscopy (XPS) measurements were recorded on a Shimadzu ESCA-3400 X-ray photoelectron spectrometer using an Mg Kα source (hν = 1253.6 eV). The binding energies were calibrated using C 1s line (284.6 eV). The surface area measurements were performed with N_2 adsorption/desorption isotherms at liquid nitrogen temperature (77 K) using automatic volumetric adsorption equipment (Belsorp-max) after dehydration under vacuum at 150 °C for 12 h. The pore volumes were calculated by a single point method at P/P_0 = 0.99 and the pore size distributions were derived from the isotherms using a non-local density functional theory (NL-DFT) method. The content of Pt and Ni in catalysts was determined by the inductively coupled plasma optical emission spectroscopy (ICP-OES) on an inductively coupled plasma analysis system (Thermo Scientific iCAP6300). Further, the contents of nitrogen in supports and catalysts were determined by the elemental analyses using PerkinElmer 2400II instruments. The Scanning

electron microscopic (SEM) analyses were carried out with a Hitachi S5000 field emission scanning electron microscope. The transmission electron microscopy (TEM), high-angle annular dark field scanning transmission electron microscopy (HAADF-STEM), and EDX spectra were recorded on FEI TECNAI G^2 F20 at an accelerating voltage of 200 kV.

4. Catalytic activity

4.1. Procedure for dehydrogenation of hydrazine hydrate. A mixture of as-prepared catalysts and aqueous solution of NaOH (0.0-5.0 mmol) in a two-neck round bottom flask was placed in a water bath at a preset temperature (298-323 K) under ambient conditions. A gas burette filled with water was connected to the reaction flask to measure the volume of the released gas at room temperature. The reaction started when hydrazine monohydrate (0.1 mL, 2.0 mmol) was injected into the flask using a syringe and volume of the evolved gas was monitored by recording the displacement of water in gas burette. The gas released during the reaction was passed through a trap containing 1.0 M hydrochloric acid to ensure the absorption of ammonia. The molar ratio of (Pt + Ni)/hydrazine were theoretically fixed at 0.05 for all the catalytic reactions.

4.2. Durability test of the catalyst. For the durability test, two different experiments were performed. One experiment was that 4.0 mmol of NaOH was only added in the first cycle, and hydrazine monohydrate (2.0 mmol) without NaOH was subsequently injected into the reactor in the following cycles. The catalyst was not recollected and washed with water during the catalytic reactions. The catalyst after 5 cycles was collected for XRD, SEM and TEM analyses. Another experiment was performed through recovering the $Pt_{0.5}Ni_{0.5}$/NGNs-850 catalyst by centrifugation and washing with water, as well as adding a fixed concentration of substrates (2.0 of mmol and 4.0 mmol of NaOH) in each cycle.

4.3. Turnover frequency (TOF) calculation. The TOF reported here is an apparent TOF value based on the number of (Pt + Ni) atoms in the catalysts, which is calculated from the equation as follows:

$$TOF = \frac{P_0 V}{1.5RTn_{PtNi}t}$$

whereas, P_0 is the atmospheric pressure (101325 Pa), V is the volume of generated gas (H_2 + N_2) at the time of half-completion of reaction, R is the universal gas constant (8.3145 m^3 Pa mol^{-1} K^{-1}), T is the reaction temperature (298-323 K), n_{PtNi} is the total number of moles of (Pt + Ni) atoms in the catalyst and t is the time in hour for half-completion of reaction.

5. Figures

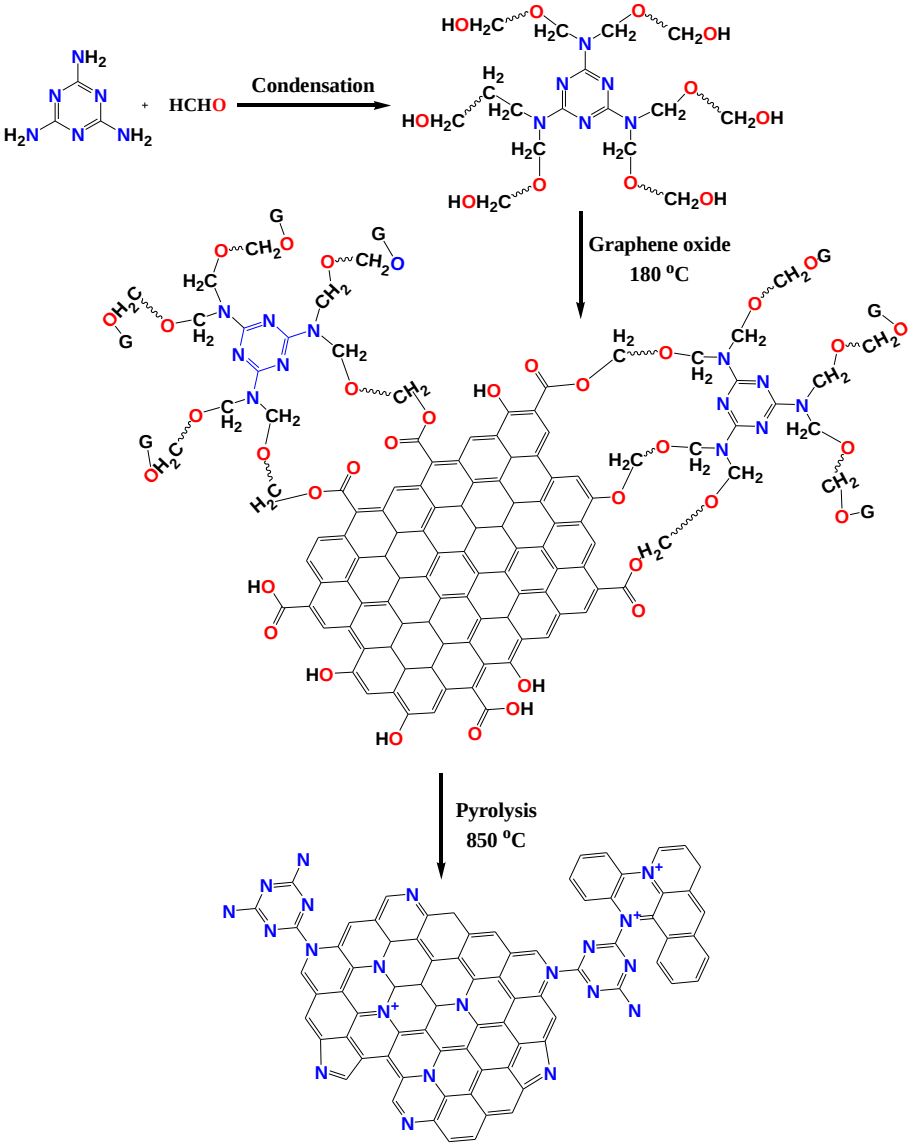

Scheme S1. Schematic illustration of the formation of 3-dimensional N-doped graphene networks (NGNs-850) via cross-linking of GO and MFR.[S2]

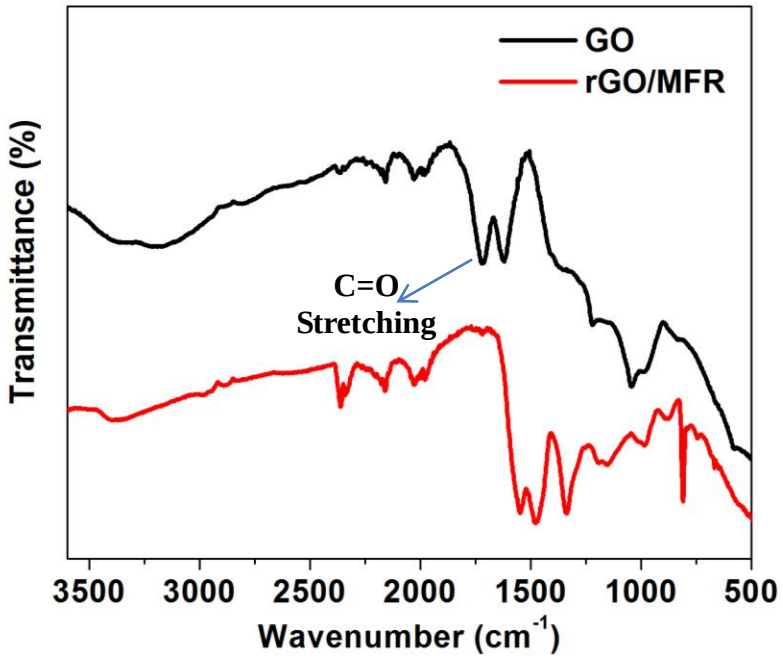

Fig. S1 IR spectra of GO and rGO/MFR implying the reduction and bonding of C=O groups of GO to MFR during hydrothermal reaction.

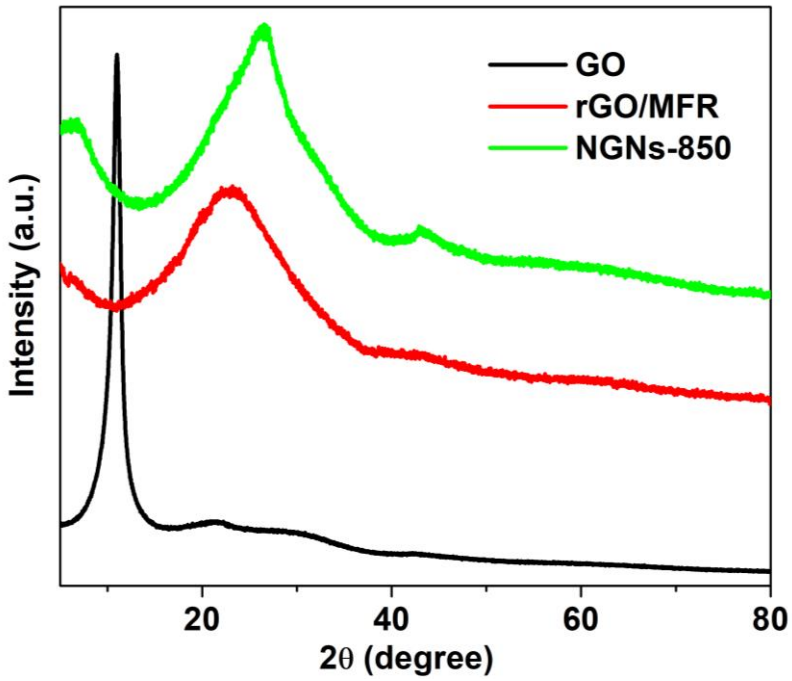

Fig. S2 PXRD pattern of GO, rGO/MFR and NGNs-850.

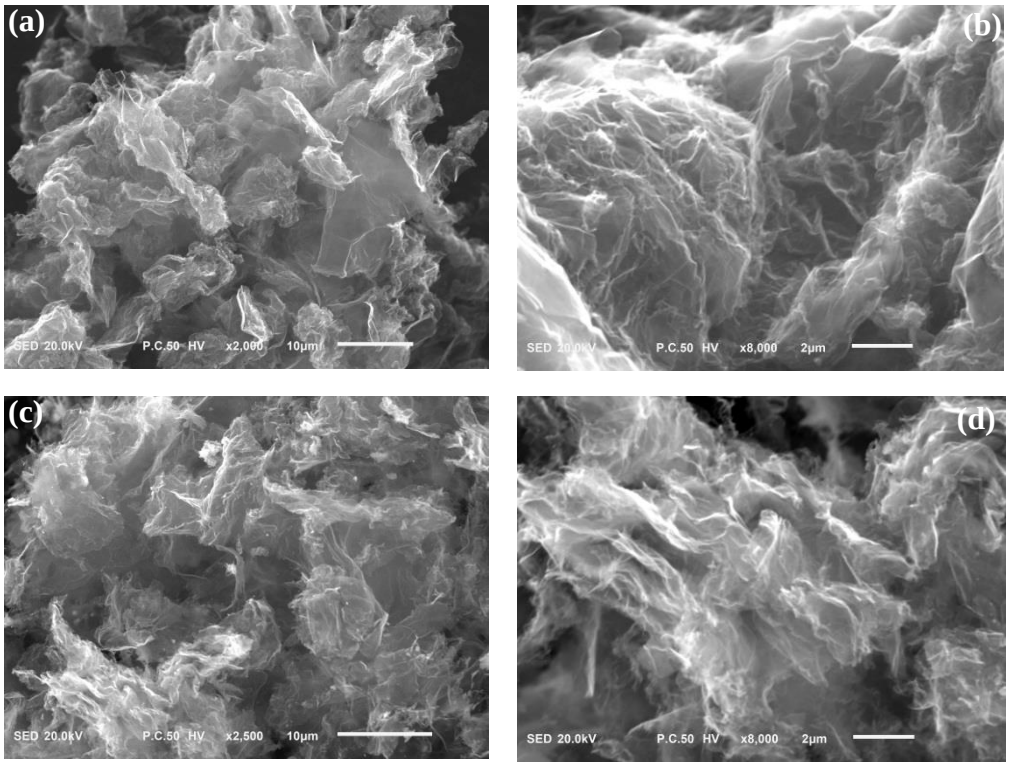

Fig. S3 SEM images of (a, b) NGNs-850 and (c, d) $Pt_{0.5}Ni_{0.5}$/NGNs-850.

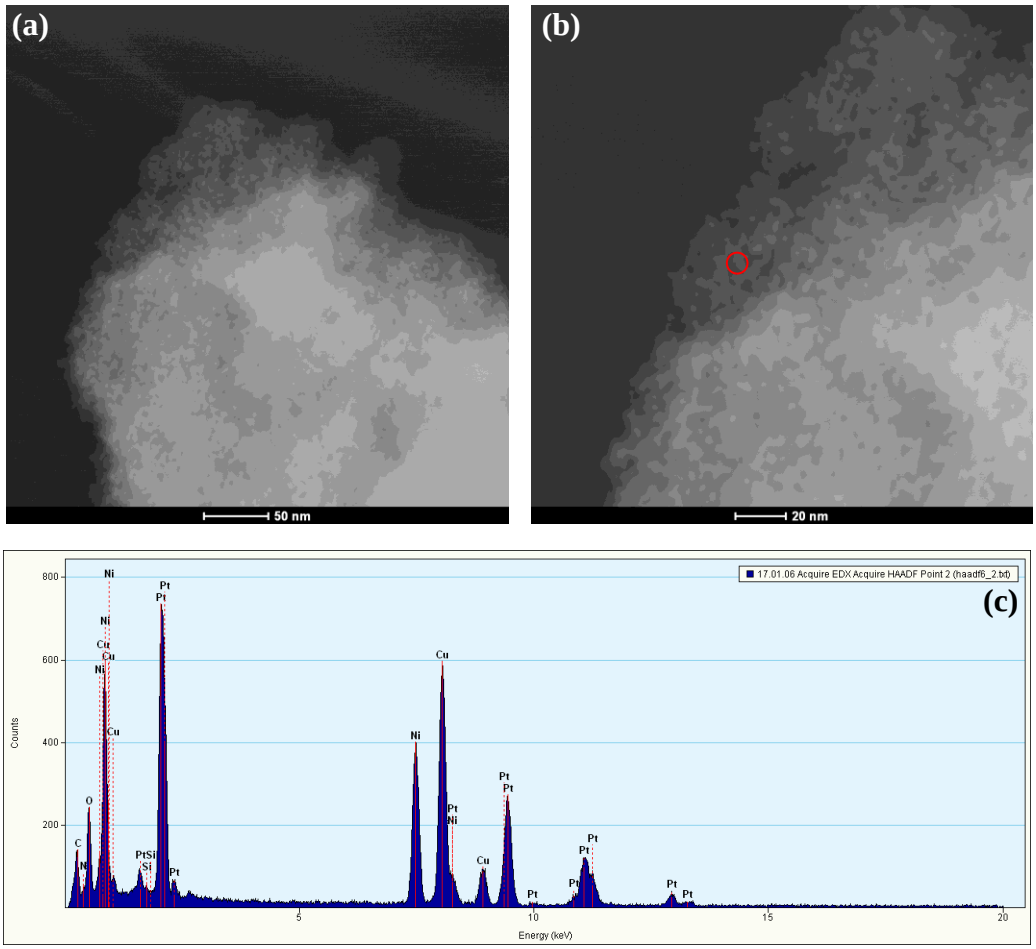

Fig. S4 (a, b) HAADF-STEM images and (c) EDX spectrum of $Pt_{0.5}Ni_{0.5}$/NGNs-850 for the selected area in fig. S5b.

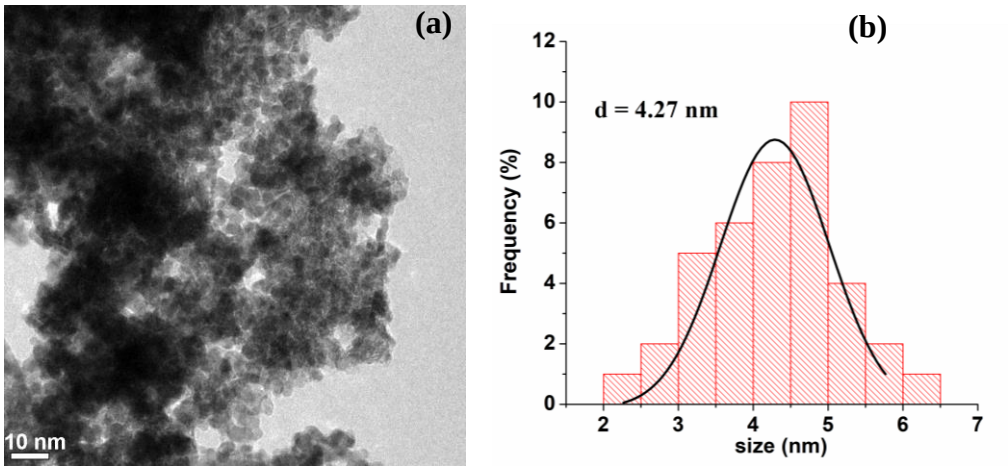

Fig. S5 (a) TEM image and (b) corresponding size histogram of $Pt_{0.5}Ni_{0.5}$/GNs.

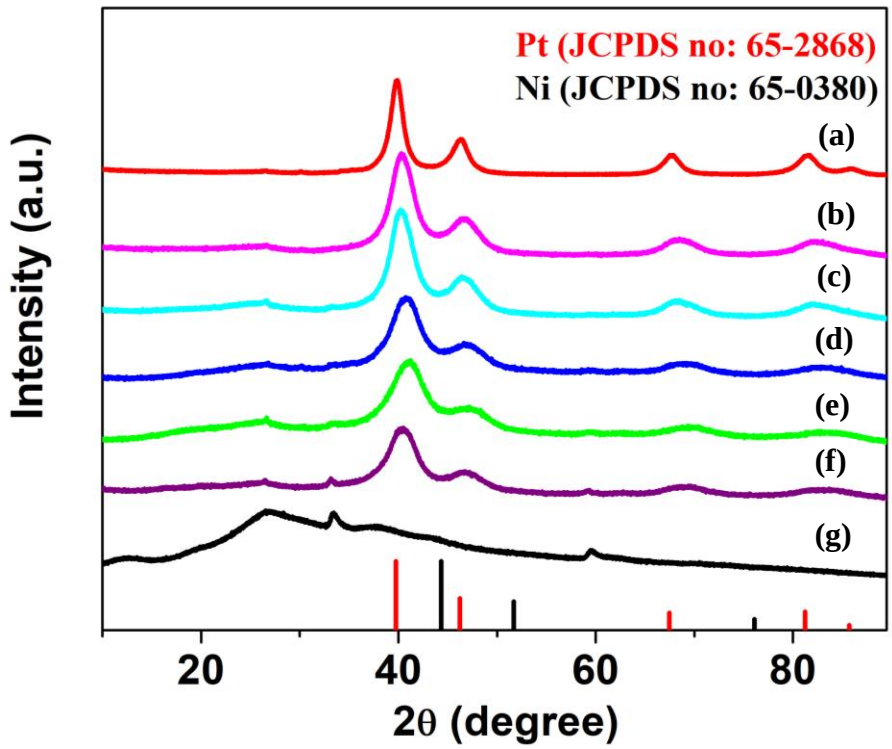

Fig. S6 PXRD patterns for Pt_xNi_{1-x}/NGNs-850 catalysts; (a) Pt/NGNs-850, (b) $Pt_{0.7}Ni_{0.3}$/NGNs-850, (c) $Pt_{0.6}Ni_{0.4}$/NGNs-850, (d) $Pt_{0.5}Ni_{0.5}$/NGNs-850, (e) $Pt_{0.4}Ni_{0.6}$/NGNs-850, (f) $Pt_{0.3}Ni_{0.7}$/NGNs-850, and (g) Ni/NGNs-850, (Red line; Pt, JCPDS no. 65-2868 and Black line; Ni, JCPDS no. 65-0380).

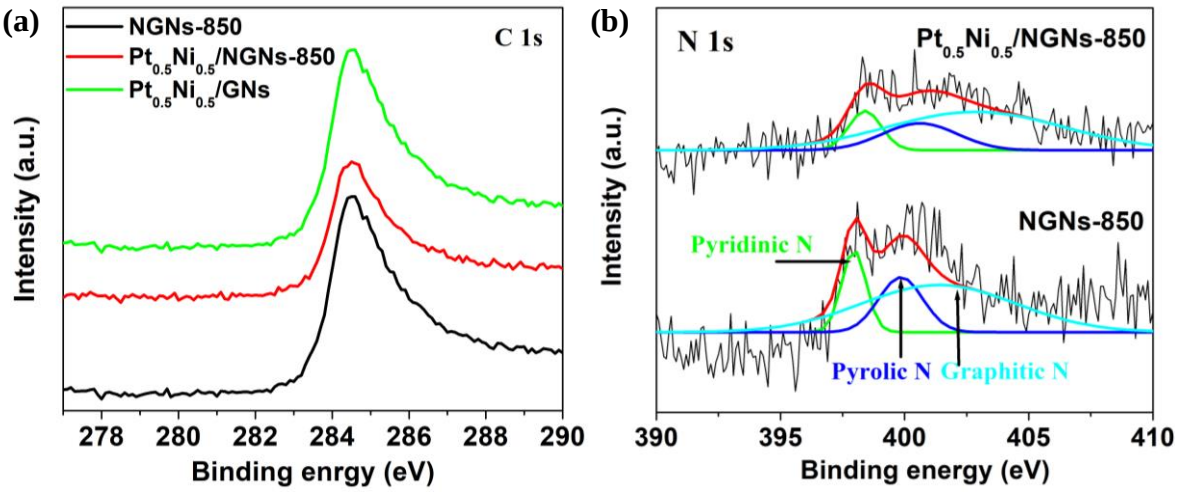

Fig. S7 XPS spectra of (a) C 1s level for NGNs-850, $Pt_{0.5}Ni_{0.5}$/NGNs-850 and $Pt_{0.5}Ni_{0.5}$/GNs and (b) N 1s level for NGNs-850 and $Pt_{0.5}Ni_{0.5}$/NGNs-850.[S2]

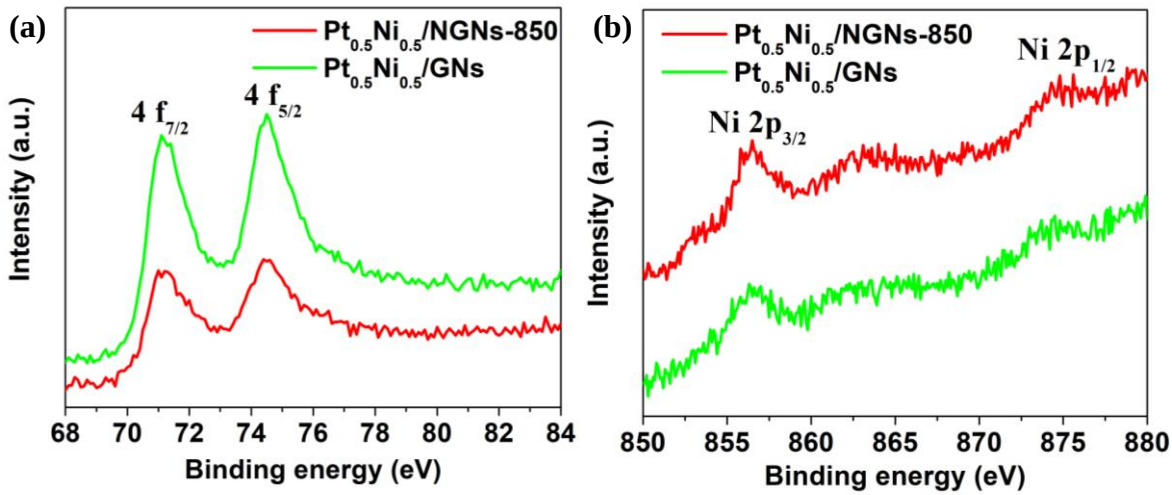

Fig. S8 XPS spectra of (a) Pt 4f level and (b) Ni 2p level for $Pt_{0.5}Ni_{0.5}$/NGNs-850 and $Pt_{0.5}Ni_{0.5}$/GNs.

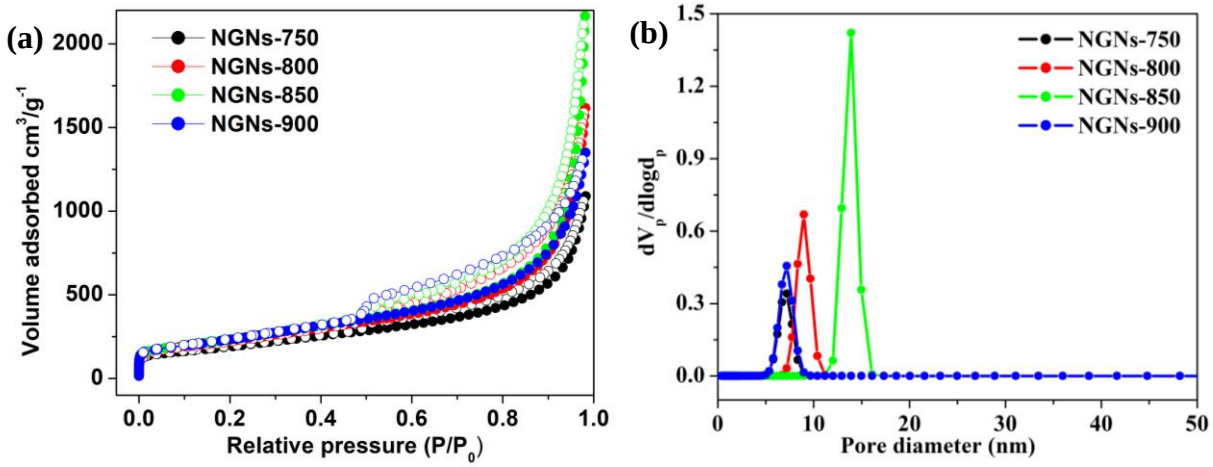

Fig. S9 (a) N_2 adsorption (filled symbols) and desorption (hollow symbols) isotherms and (b) Non-local density functional theory (NLDFT) pore size distributions for as-synthesized NGNs-750, NGNs-800, NGNs-850 and NGNs-900 supports at 77 K.

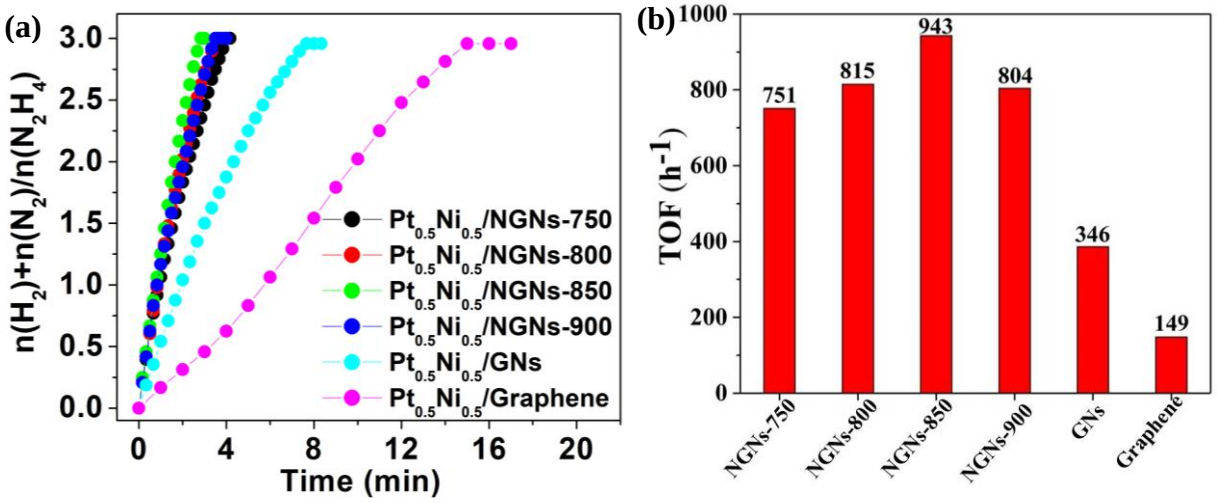

Fig. S10 (a) Volume of the generated gas (H_2 + N_2) *versus* time and (b) corresponding TOF values for the dehydrogenation of hydrazine monohydrate over $Pt_{0.5}Ni_{0.5}$ catalysts on different supports at 303 K ($n_{metal}/n_{hydrazine}$ = 0.05, n_{NaOH} = 4 mmol).

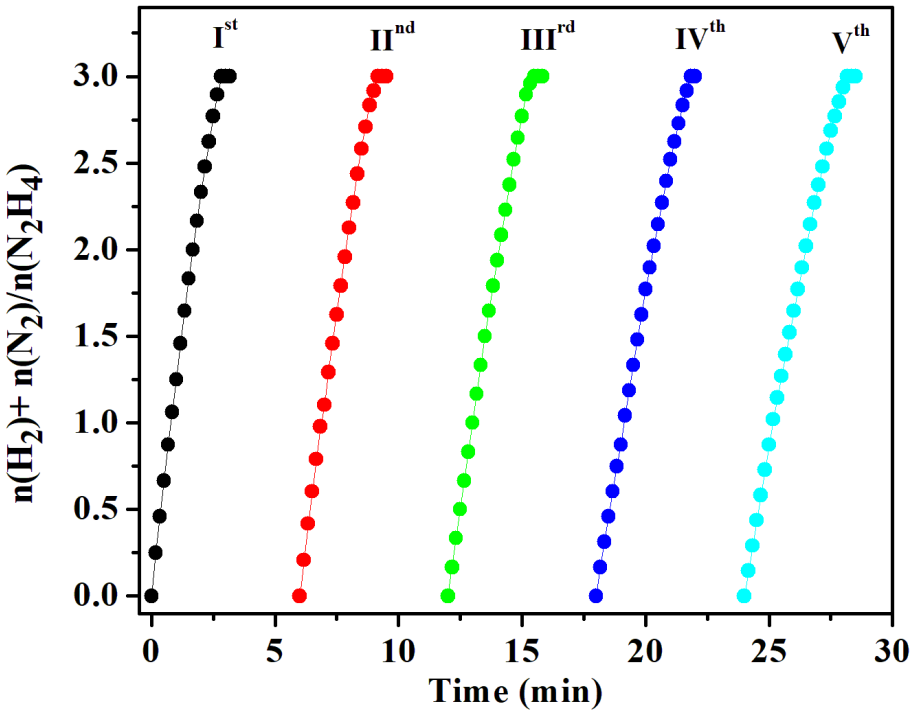

Fig. S11 Durability test toward dehydrogenation of hydrazine monohydrate over $Pt_{0.5}Ni_{0.5}$/NGNs-850 catalyst through adding 4.0 mmol of NaOH in the first cycle, as well as adding hydrazine (without NaOH) in the following cycles.

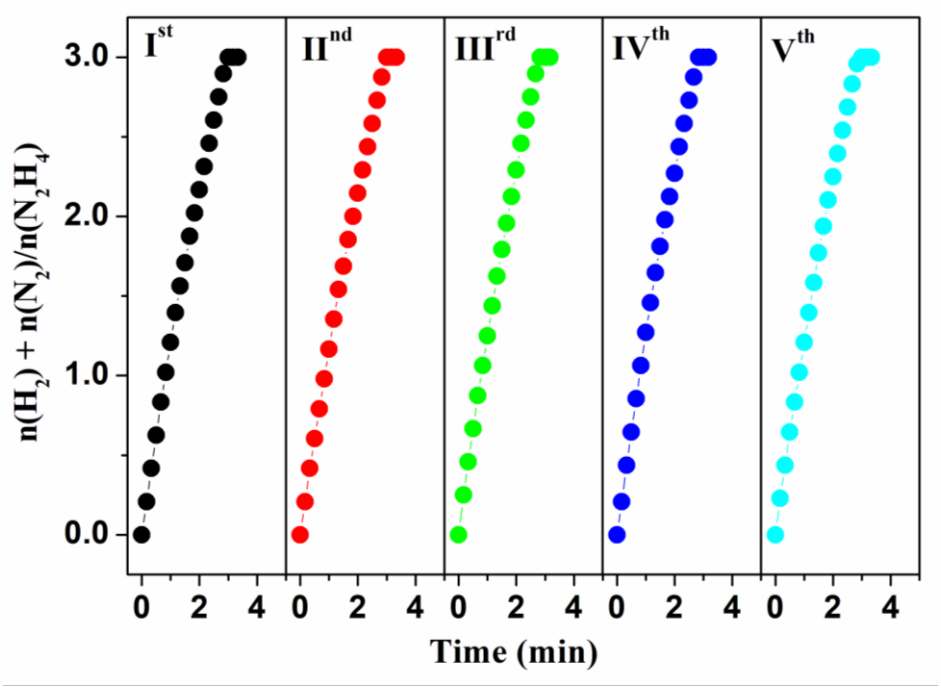

Fig. S12 Durability test toward dehydrogenation of hydrazine monohydrate through recovering the $Pt_{0.5}Ni_{0.5}$/NGNs-850 catalyst by centrifugation and washing with water in each cycle, as well as adding the substrates with a fixed concentration (2.0 mmol of hydrazine and 4.0 mmol of NaOH) in each cycle.

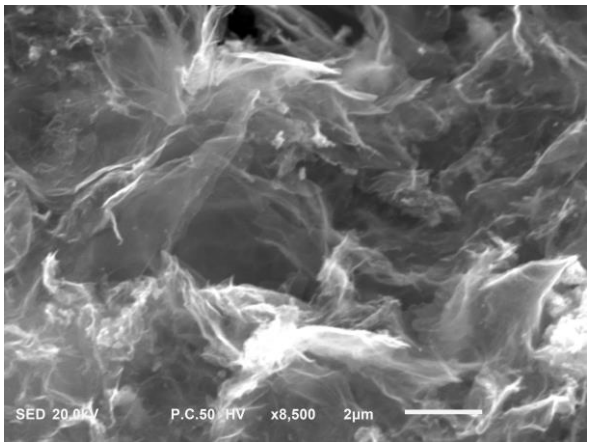

Fig. S13 SEM images of $Pt_{0.5}Ni_{0.5}$/NGNs-850 catalyst recovered after 5 cycles.

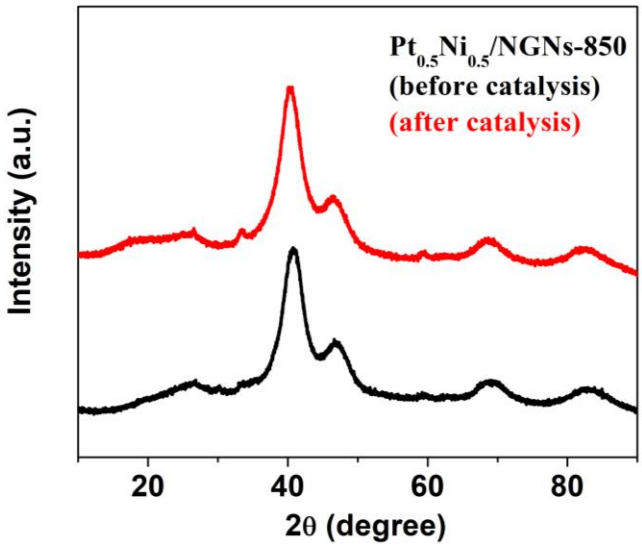

Fig. S14 XRD pattern of $Pt_{0.5}Ni_{0.5}$/NGNs-850 catalyst before (black) and after (red) 5 cycles.

6. Tables

Table S1. Catalytic activity of $Pt_{0.5}Ni_{0.5}$/NGNs-850 toward dehydrogenation of hydrazine compared to other reported catalysts.

Catalyst	Solvent Medium	Temp (K)	Selectivity for H_2 (%)	TOF (h^{-1})	E_a (KJ mol^{-1})	Reference
$Pt_{0.5}Ni_{0.5}$/NGNs-850	Aqueous NaOH	323	100	2116	32.28	Present
		303		943		work
$Pt_{0.6}Ni_{0.4}$/PDA-rGO	Aqueous NaOH	323	100	2056	33.39	S3
		303		903		
$(Ni_3Pt_7)_{0.5}$-$(MnO_x)_{0.5}$/NPC-900	Aqueous NaOH	323	100	706	50.15	S4
		298		120		
$Ni_{84}Pt_{16}$/graphene	Aqueous NaOH	323	100	415	40.4	S5
		298		133		
Ni_3Pt_7/graphene	Aqueous NaOH	323	100	415	49.36	S6
RhNiP/rGO	Aqueous NaOH	323	100	471	40.4	S7
PtNi/C	Aqueous NaOH	323	100	210	55.3	S8
$Ni_{0.6}Fe_{0.4}B$	Aqueous NaOH	323	100	28.8	50.7	S9
$Pt_{60}Ni_{40}$-CNDs	Aqueous NaOH	323	100	170	43.9	S10
Ni_6Pt_4-SF	Aqueous NaOH	298	100	150	-	S11
$Ni_{0.9}Pt_{0.1}/Ce_2O_3$	Aqueous NaOH	298	100	28.1	42.3	S12
$Rh_{4.4}Ni$/graphene	Aqueous NaOH	298	100	28	-	S13
Ni_3Fe/C	Without additive	293	100	528	48.1	S14
$NiIr_{0.059}/Al_2O_3$-HT	Without additive	303	99	12.4	49.3	S15
$NiPt_{0.057}/Al_2O_3$-HT	Without additive	303	97	16.5	34	S16
$Ni_{1.5}Fe_{1.0}/(MgO)_{3.5}$	Without additive	299	99	11	-	S17
Rh	Without additive	298	43.8	2.5	-	S18
Rh4Ni	Without additive	298	100	4.8	-	S19
$Ni_{0.95}Ir_{0.05}$	Without additive	298	100	2.2	-	S20

Table S2. Elemental analyses for NGNs-850 and $Pt_{0.5}Ni_{0.5}$/NGNs-850 catalysts.

Sample	N (wt. %)
NGNs-850	5.8
$Pt_{0.5}Ni_{0.5}$/NGNs-850	2.8

Table S3. ICP analyses for the catalysts.

Sample	Pt (wt. %)	Ni (wt. %)
$Pt_{0.5}Ni_{0.5}$/NGNs-850	38	13
$Pt_{0.5}Ni_{0.5}$/GNs	35	11

Table S4. BET surface areas and pore volumes for the prepared samples.

Sample	S_{BET} (m^2 g^{-1})	Pore volume (cm^3 g^{-1})
NGNs-750	691	1.685
NGNs-800	819	2.50
NGNs-850	860	3.349
NGNs-900	862	2.088
$Pt_{0.5}Ni_{0.5}$/NGNs-850	365	0.672

References

(S1) (a) W. S. Hummers and R. E. Offeman, *J. Am. Chem. Soc*., 1958, **80**, 1339; (*b*) Y. Chen, X. Zhang, P. Yu and Y. Ma, *Chem. Commun*., 2009, 4527.

(S2) Y. Qin, J. Yuan, J. Li, D. Chen, Y. Kong, F. Chu, Y. Tao and M. Liu, *Adv. Mater*., 2015, **27**, 5171.

(S3) F.-Z. Song, Q.-L. Zhu and Q. Xu, *J. Mater. Chem. A*, 2015, **3**, 23090.

(S4) B. Xia, T. Liu, W. Luo and G. Cheng, *J. Mater. Chem. A*, 2016, **4**, 5616.

(S5) Y. Du, J. Su, W. Luo and G. Cheng, *ACS Appl. Mater. Interfaces*, 2015, **7**, 1031.

(S6) N. Cao, L. Yang, C. Du, J. Su, W. Luo and G. Cheng, *J. Mater. Chem. A*, 2014, **2**, 14344.

(S7) X. Du, S. Tan, P. Cai, W. Luo, G. Cheng, *J. Mater. Chem. A*, 2016, **4**, 14572.

(S8) S. N. Oliaee, C. Zhang, S. Y. Hwang, H. M. Cheung and Z. Peng, *J. Phys. Chem. C*, 2016, **120**, 9764.

(S9) H. L. Wang, J. M. Yan, S. J. Li, X. W. Zhang and Q. Jiang, *J. Mater. Chem. A.*, 2015, **3**, 121.

(S10) J. K. Sun and Q. Xu, *ChemCatChem*, 2015, **7**, 526.

(S11) A. K. Singh and Q. Xu, *Int. J. Hydrog. Energy*, 2014, **39**, 9128.

(S12) H. L. Wang, J. M. Yan, W. L. Wang, O. Song-Il and Q. Jiang, *J. Mater. Chem. A.*, 2013, **1**, 14957.

(S13) J. Wang, X. B. Zhang, Z. L. Wang and Y. Zhang, *Energy Environ. Sci*., 2012, **5**, 6885.

(S14) D. G. Tong, D. M. Tang, W. Chu, G. F. Gu and P. Wu, *J. Mater. Chem. A.*, 2013, **1**, 6425.

(S15) L. He, Y. Huang, X. Liu, L. Lin, A. Wang, X. Wang, C. Y. Mou and T. Zhang, *Appl. Catal. B*, 2014, **147**, 779.

(S16) L. He, Y. Huang, A. Wang, Y. Liu, X. Liu, X. Chen, J. J. Delgado, X. Wang and T. Zhang, *J. Catal*., 2013, **298**, 1.

(S17) W. Gao, C. Li, H. Chen, M. Wu, S. He, M. Wei, D. Evans and X. Duan, *Green Chem.* 2014, **16**, 1560.

(S18) S. K. Singh, X. B. Zhang and Q. Xu, *J. Am. Chem. Soc*., 2009, **131**, 9894.

(S19) S. K. Singh and Q. Xu, *J. Am. Chem. Soc*., 2009, **131**,18032.

(S20) S. K. Singh and Q. Xu, *Chem. Commun*., 2010, **46**, 6545.